

Article

Rare Earth Element Characteristics in Coal Ash from the Jungar Energy Gangue Power Plant, Inner Mongolia, China

Shaoqing Huang¹, Shuzheng Ning^{1,*}, Degao Zhang^{1,2}, Yuan Cai³, Xiaoyun Yan¹, Kang Liu¹ and Xiaotao Xu¹¹ General Prospecting Institute of China National Administration of Coal Geology, Beijing 100039, China² China National Administration of Coal Geology, Beijing 100038, China³ Beijing Pan Land Ocean Energy Technology Research Institute, Beijing 100089, China

* Correspondence: nsz0321@126.com

Abstract: The coal and coal-bearing measures in the Jungar Coalfield in Inner Mongolia are characterized by rare earth element (REE) enrichment. Combustion in coal-fired power plants can lead to further enrichment of REEs in coal ash, which serves as a new potential source for REE extraction and smelting. Further, investigating the content, modes of occurrence, and transformation behavior of REEs during coal combustion may help in better understanding REE differentiation during coal combustion and facilitate the development of economically feasible REE recovery technologies. Therefore, in this study, we analyzed coal ash from the Jungar Energy Gangue Power Plant in Inner Mongolia via inductively coupled plasma mass spectrometry, X-ray diffraction, and scanning electron microscopy combined with energy-dispersive spectroscopy. Our results showed that the REE content of the feed coal was 220 µg/g, slightly higher than the average for global coal. Additionally, fly ash had a higher REE content (898 µg/g) than bottom ash, and its rare earth oxide content was approximately 1152 µg/g, which meets the industrial requirements. Bottom and fly ashes contained similar minerals; however, their relative abundances were different. Specifically, mullite, quartz, calcite, and gypsum were slightly more abundant in fly ash than in bottom ash, whereas amorphous solids were slightly more abundant in bottom ash than in fly ash. Furthermore, fly ash, dominated by Si- and Al-rich minerals, was composed of irregular particles of different shapes and sizes. It also contained monazite and REE fluoro-oxides, which possibly originated from the feed coal and had mineral structures that remained unchanged during coal combustion. Thus, the REE fluoro-oxides possibly resulted from the conversion of bastnaesite in the feed coal during combustion and thereafter became attached to the edge of the Si–Al minerals in the fly ash.

Keywords: Jungar Coalfield; coal ash; rare earth elements; fly ash; differentiation; REE minerals

Citation: Huang, S.; Ning, S.; Zhang, D.; Cai, Y.; Yan, X.; Liu, K.; Xu, X. Rare Earth Element Characteristics in Coal Ash from the Jungar Energy Gangue Power Plant, Inner Mongolia, China. *Minerals* **2023**, *13*, 1212. <https://doi.org/10.3390/min13091212>

Academic Editors: Shifeng Dai and Alexandra Guedes

Received: 27 June 2023

Revised: 12 September 2023

Accepted: 13 September 2023

Published: 15 September 2023



Copyright: © 2023 by the authors. Licensee MDPI, Basel, Switzerland. This article is an open access article distributed under the terms and conditions of the Creative Commons Attribution (CC BY) license (<https://creativecommons.org/licenses/by/4.0/>).

1. Introduction

Rare earth elements (REEs), which are also often referred to as “industrial gold”, are widely used in military applications, communications technology, new energy development, petrochemical processing, metallurgy, modern agriculture, and other commercial fields owing to their excellent physical properties. Further, they constitute an irreplaceable resource for upgrading and modernizing industry. They have also become a strategic mineral resource of China [1–3]. At their peak, China’s REE reserves accounted for 71.1% of the global total; however, this share has dropped sharply to <34% [4,5]. Therefore, the identification of new REE sources has become a priority. In this study, REEs refer to the lanthanides, scandium (Sc), and yttrium (Y).

The formation of coal, which is an organic-rich rock, is characterized by reduction and adsorption barriers, and under certain coupling conditions, coal-bearing series can concentrate a variety of metals [6–12], offering the possibility of recovering critical elements from coal and coal ash [13–16]. In recent years, the abundance, origin, and modes of occurrence of critical elements in coal have been investigated [17–24], and all these studies

have shown that coal is a promising source of critical metals [25–29]. The Jungar Coalfield in Inner Mongolia is a typical area for metal element enrichment in coal measures [30–35] and could potentially serve as a new source of REEs.

Further, coal ash, which generally includes fly ash and bottom ash, is a byproduct of coal combustion in coal-based power plants. As most of the organic matter in coal is lost after combustion, REEs are further enriched in coal ash [36–39]. Specifically, fly ash, which is fine and light, flies into the smokestacks of power plants and is captured using filters, while bottom ash is heavy, clumps, and settles at the bottom of the furnace. Owing to the differences in their properties, the metallic elements in coal ash differ between fly and bottom ashes.

Generally, there are two types of coal-fired generator set boilers based on different combustion methods, namely pulverized coal furnaces and circulating fluidized bed (CFB) boilers. Specifically, the combustion temperature in CFB boilers varies in the range of 800–950 °C, while the flame temperature in pulverized coal boilers is as high as 1300–1700 °C. Further, the characteristics of the coal ash resulting from these different boilers with different combustion temperatures are considerably different.

Hower et al. [10] studied the distribution characteristics of REEs in fly ash from different regions, and Dai et al. [40] and Zhao et al. [41] studied the mineral characteristics and differentiation of REEs in fly ash from the Junge Power Plant (with a pulverized coal furnace) using Hedaigou coal as fuel. Although Hedaigou coal is also used as fuel in the Jungar Energy Gangue Power Plant, the minerals and REE differentiation characteristics of its fly ash are different from those of the coal ash from the Junge Power Plant [40].

In this study, the distribution and differentiation characteristics of REEs in feed coal, fly ash, and bottom ash from the Jungar Energy Gangue Power Plant were investigated. The mineral characteristics of fly ash and the possible behavioral characteristics of REEs during the combustion process were also examined to provide a reference for the utilization of REEs present in fly ash.

2. Materials and Methods

2.1. Overview of the Study Area

The Jungar Coalfield is located in the northeastern margin of the Ordos Basin in Inner Mongolia, China [42–45]. The coal measure strata in this coalfield comprise the Taiyuan Formation of the Upper Carboniferous (C_{3t}) and main coal seam No. 6. The main sources of the elements in the coal are the middle Proterozoic potassium feldspar granite of the Yinshan Paleoland and the weathering crust of the Benxi Formation. The REE content of coal from the Heidaigou coal mine varies in the range of 54.57–559 µg/g, with the mean content being 248 µg/g (2.83-fold higher than the average content of REEs in Chinese coal) [35,46,47].

The Jungar Energy Gangue Power Plant is located in Xuejiawan, Jungar County, Inner Mongolia, northern China. At this power plant, a DG480/13.73-II11 CFB combustion boiler (Dongfang Boiler Company, Sichuan, China) is used, and the fuel is coal from the No. 6 coal seam of the Taiyuan Formation [48,49] in the Heidaigou open-pit mine (Figure 1), with an ash yield of approximately 20%. Further, the combustion temperature in this boiler is between 850 and 900 °C.



Figure 1. Distribution of mining areas in the Jungar Coalfield, modified from reference [35].

2.2. Sample Collection and Analysis Methods

2.2.1. Sample Collection and Preparation

The samples were collected from the same batches of feed coal, fly ash from an electrostatic precipitator, and bottom ash. After cooling, the fly and bottom ash samples were collected under normal boiler operating conditions and stored in sealed bags. Feed coal was collected from the coal storage yard of the power plant. To ensure that the samples were representative, we collected and mixed feed coal samples from five evenly distributed points in the coal pile before analysis.

2.2.2. Elemental and Mineralogical Analysis

The feed coal, fly ash, and bottom ash samples were analyzed for moisture and fixed carbon and sulfur contents. Their loss on ignition (LOI) values were also determined via heating at 815 °C for at least 1 h. Further, the feed coal samples were analyzed for ash yield. The analyses were performed according to Chinese National Standard GB/T 212-2008.

An Axios-Max X-ray fluorescence spectrometer (XRF) was used to determine the contents of the oxides of major elements, including SiO₂, TiO₂, Al₂O₃, Fe₂O₃, MgO, CaO, Na₂O, K₂O, SO₃, MnO₂, and P₂O₅, in the high-temperature (815 °C) samples of the feed coal, fly ash, and bottom ash. This analysis of oxide contents was performed according to Chinese National Standard GB/T 21114-2019.

The mineral contents of the feed coal, fly ash, and bottom ash samples were quantified via powder X-ray diffraction (XRD). The feed coal and bottom ash samples were crushed and sieved through a 200-mesh sieve for XRD analysis using an XD3 XRD analyzer. The XRD patterns of the samples were recorded over a 2θ interval of 2°–70° with a step size of 0.02° in accordance with Chinese Petroleum and Gas Standard SY/T 6210-1996.

A 300X inductively coupled plasma mass spectrometer (ICP-MS) was used to measure the REE and trace element contents of the feed coal, fly ash, and bottom ash samples, which

were first subjected to microwave digestion in ultrapure concentrated HNO₃ using high-pressure quartz vessels. These analyses were performed according to Chinese National Standard GB/T 14506.30-2010.

A Vega II LMU band energy spectrometer and a scanning electron microscope (SEM–EDX) were used for morphological observations and to determine the microscopic appearance and major elemental composition of the minerals in the feed coal, fly ash, and bottom ash samples. The samples were carbon coated to increase their conductivity.

3. Results and Discussion

3.1. Properties

Table 1 lists the moisture content, ash yield, fixed carbon and sulfur contents, and loss on ignition (LOI) values of the samples from the Jungar Energy Gangue Power Plant. The feed coal samples have a low sulfur content (0.42%), a medium ash yield (26.54%), a fixed carbon content (44.37%), and an LOI of 72.16%. The fixed carbon contents of the fly ash and bottom ash samples were 4.09 and 6.21%, respectively. The feed particle size of the CFB boiler is large (≤ 10 mm), and the unburned carbon particles maintain a certain particle size as well as a high density. Thus, they were easily discharged with bottom ash. The LOI values of the fly ash and bottom ash samples were 7.49 and 7.55%, respectively, and were mainly related to the carbon and moisture contents of the samples.

Table 1. Moisture content, fixed carbon and sulfur contents, ash yield, and loss on ignition values for samples from the Jungar Energy Gangue Power Plant (wt.%).

Sample	M _{ad}	A _d	Fc _d	St _d	LOI
Feed coal	5.00	26.54	44.37	0.42	72.16
Fly ash	0.60	\	4.09	0.18	7.49
Bottom ash	0.12	\	6.21	0.22	7.55

Note: M, moisture; ad, air dry basis; A, ash; d, dry basis; Fc, fixed carbon; St, total sulfur; LOI, loss on ignition; \, no data.

3.2. Chemistry

3.2.1. Chemistry of Feed Coal

Table 2 lists the contents and characteristics of the elements in the feed coal and coal ash samples from the Jungar Energy Gangue Power Plant. The concentration coefficient (CC) proposed by Dai et al. [50] was used for the evaluation (CC = the ratio of element concentration in investigated coal samples to element concentration in global hard coal samples [51]; $10 < CC < 100$, significantly enriched; $5 < CC < 10$, enriched; $2 < CC < 5$, slightly enriched; $0.5 < CC < 2$, normal; $CC < 0.5$, depleted). For Eu, Gd, Ho, Tm, and Lu, the CCs varied between 2 and 4, while the overall CC of the REEs was 2.78, indicating an enrichment. The SiO₂ and Al₂O₃ contents of the feed coal exceeded the global coal average. Specifically, the Al₂O₃ content was 2.26 times the global coal average, while the Fe₂O₃ and CaO contents were far less than the global coal average (Figure 2).

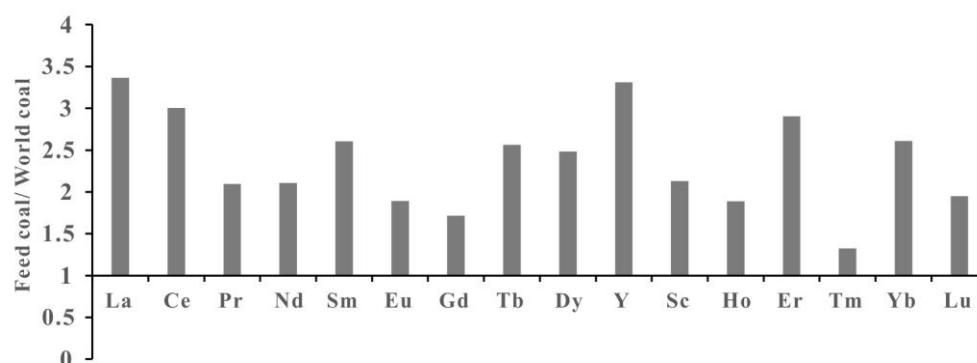


Figure 2. Coal enrichment coefficients for feed coal from the Jungar Energy Gangue Power Plant.

Table 2. Concentrations of major element oxides (%) and REEs (µg/g) in feed coal and coal combustion products from the Jungar Energy Gangu Power Plant.

Sample	Feed Coal	Bottom Ash	Fly Ash	Differentiation Coefficient (DC)	Global Coal	Concentration Coefficient (CC)
SiO ₂	12.07	46.39	37.55	0.81	8.47	1.43
TiO ₂	0.33	0.69	1.20	1.74	0.33	1.00
Al ₂ O ₃	13.49	46.42	52.24	1.13	5.98	2.26
Fe ₂ O ₃	0.47	3.52	1.39	0.39	4.85	0.10
MgO	0.10	0.10	0.54	5.40	0.22	0.45
CaO	0.72	1.82	3.58	1.97	1.23	0.59
Na ₂ O	0.05	0.10	0.18	1.80	0.16	0.31
K ₂ O	0.10	0.29	0.43	1.48	0.19	0.53
SO ₃	0.60	0.34	0.88	2.56	\	\
MnO ₂	0.006	0.01	0.02	2.00	\	\
P ₂ O ₅	0.005	0.05	0.24	4.80	\	\
La	37.00	42.30	181.00	4.28	11.00	3.36
Ce	69.10	79.60	325.00	4.08	23.00	3.00
Pr	7.33	9.16	34.80	3.80	3.50	2.09
Nd	25.30	30.20	116.00	3.84	12.00	2.11
Sm	5.21	5.32	23.40	4.40	2.00	2.61
Eu	0.89	0.95	3.99	4.20	0.47	1.89
Gd	4.63	4.79	19.60	4.09	2.70	1.71
Tb	0.82	0.83	3.24	3.90	0.32	2.56
Dy	5.21	5.07	20.70	4.08	2.10	2.48
Y	27.80	24.90	112.00	4.50	8.40	3.31
Sc	8.31	10.05	32.70	3.25	3.90	2.13
Ho	1.02	0.96	3.88	4.04	0.54	1.89
Er	2.70	2.58	9.68	3.75	0.93	2.90
Tm	0.41	0.40	1.45	3.63	0.31	1.32
Yb	2.61	2.56	9.27	3.62	1.00	2.61
Lu	0.39	0.39	1.36	3.49	0.20	1.95
REE	198	220	898	4.08	72.37	2.75

Note: The average elemental content of global coal was based on a previous study [51]; \, no data.

3.2.2. Distribution of REEs in Fly Ash and Bottom Ash

The total REE content in fly ash was 898 µg/g, which was 1152 µg/g when expressed in terms of rare earth oxides (REOs). According to the Chinese geological and mineral industry standard “Specifications for rare earth mineral exploration (DZ/T 0204-2022)”, this content exceeds the minimum industrial grade requirement for an REE deposit. Further, the REE content of bottom ash was 220 µg/g. Thus, the REEs showed clear differentiation between fly ash and bottom ash, and the differentiation coefficient (DC) [52] (DC = ratio of the elemental content of fly ash to that of bottom ash) was used to characterize the degree of differentiation (Table 2, Figure 3). The DC of the REEs was approximately 4; i.e., the REE content in the fly ash samples was four times that in the bottom ash samples, indicating that after combustion, REEs were predominantly enriched in fly ash.

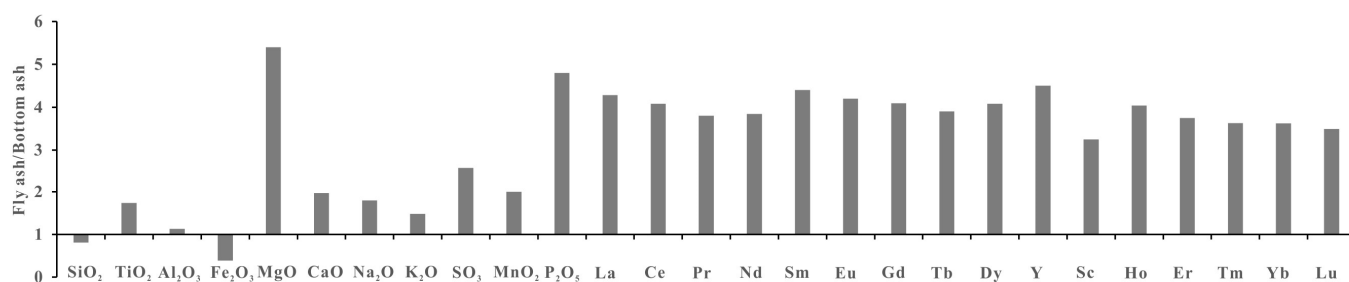


Figure 3. Differentiation characteristics of coal ash from the Jungar Energy Gangu Power Plant.

The REE content of the coal sample (ash basis) was used to standardize the REE content of the fly and bottom ashes (Figure 4). The pattern of REEs in the fly ash was right-skewed, and relative to heavy REEs (including Sc and Y), light REEs tended to migrate into fly ash after combustion.

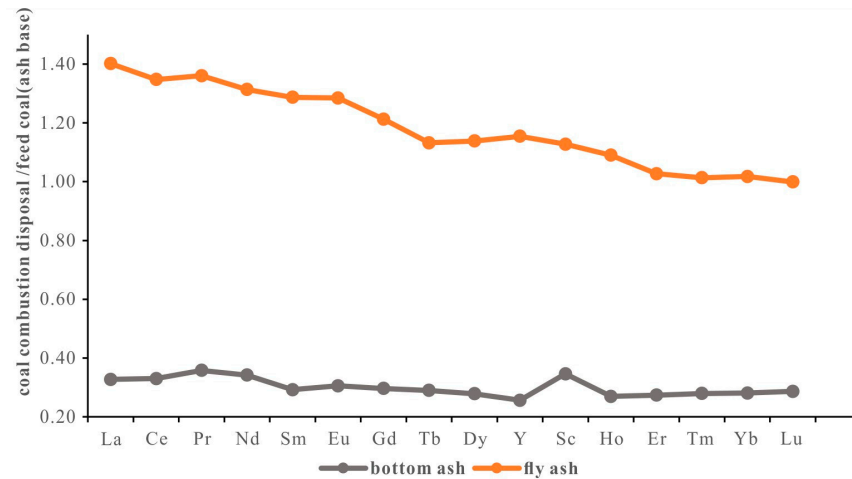


Figure 4. Diagram showing the distribution pattern of REEs in coal ash samples (standardized based on REEs (ash-based) in coal).

3.2.3. Distribution of Major Elements in Fly Ash and Bottom Ash Samples

The sum of the SiO_2 and Al_2O_3 contents of the coal ash samples (fly ash and bottom ash samples) was approximately 90%, indicative of coal ash with a high silica–aluminum content. Specifically, the Al_2O_3 contents of the bottom ash samples were above 45% and above 50% in the fly ash samples. This could be attributed to the high kaolinite and boehmite contents of the feed coal (from the Heidaigou mine). Further, the Al_2O_3 content of bottom ash was less than that of fly ash, indicating that the Al_2O_3 originating from minerals in coal during combustion was more easily discharged with fly ash. The Fe_2O_3 content of bottom ash was 3.52%, 2.5-fold higher than that of fly ash (1.39%). This is because Fe_2O_3 in the coal ash is generally converted from pyrite during combustion, and hematite (Fe_2O_3) has a higher density and is more likely to fall into bottom ash after combustion. Additionally, the CaO and SO_3 contents of fly ash were higher than those of bottom ash; this may be related to the greater ease of discharge of sulfur fixation products (CaSO_4) into fly ash. Further, Ti, Mg, P, K, and Na tended to migrate into fly ash (Table 2, Figure 3).

3.3. Mineral Characteristics

3.3.1. Feed Coal Minerals

The mineral composition of feed coal is an important factor that affects the composition of coal ash. Kaolinite (Table 3, Figures 5 and 6a) was the main mineral in the feed coal, accounting for 74.7% of the total mineral content, followed by boehmite (10.2%), calcite (6.8%; Figure 6b), gypsum (5.1%; Figure 6c), and other minor minerals. This is consistent with the previously reported mineral composition for coal from the Heidaigou coal mine [46–48,53]. REE-bearing minerals, including bastnasites (Figure 6d) and monazite (Figure 6e,f), were also found in the coal samples from the Jungar Coalfield [35].

Table 3. Mineral composition of feed coal samples from the Jungar Energy Gangue Power Plant (%).

	Kaolinite ($\text{H}_2\text{Al}_2\text{O}_8$ $\text{Si}_2 \cdot \text{H}_2\text{O}$)	Boehmite (AlOOH)	Pyrite (FeS)	Quartz (SiO_2)	Calcite (CaCO_3)	Gypsum (CaSO_4 $2\text{H}_2\text{O}$)
Feed coal	74.7	10.2	1.9	1.3	6.8	5.1

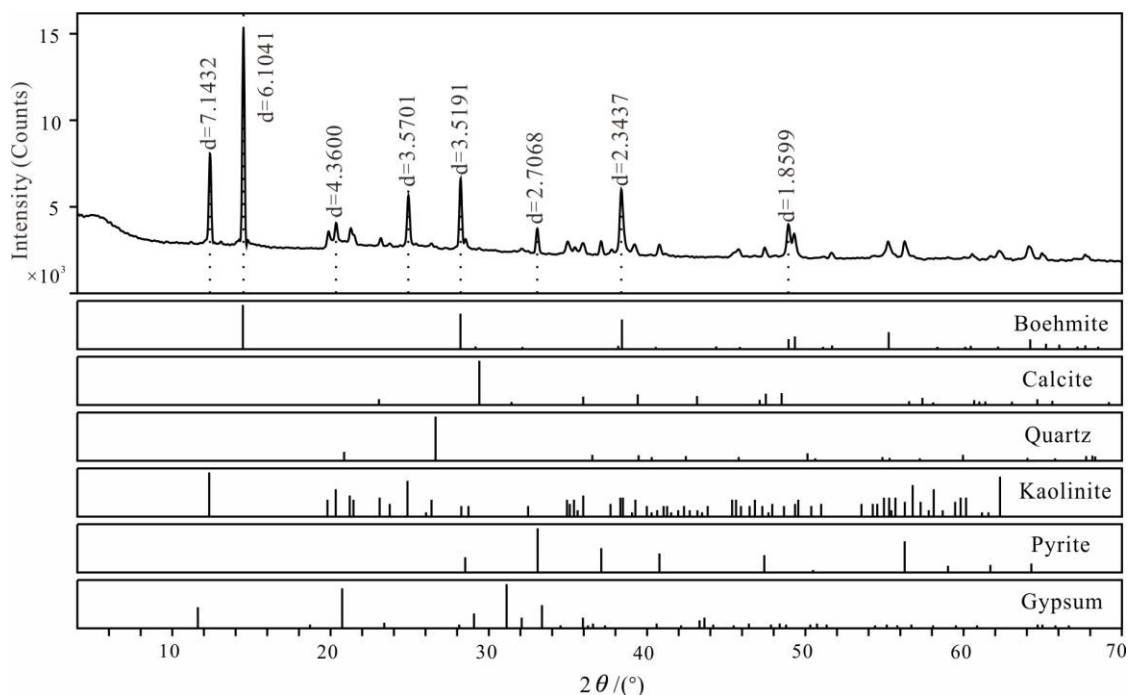


Figure 5. XRD spectrum of feed coal from the Jungar Energy Gangue Power Plant.

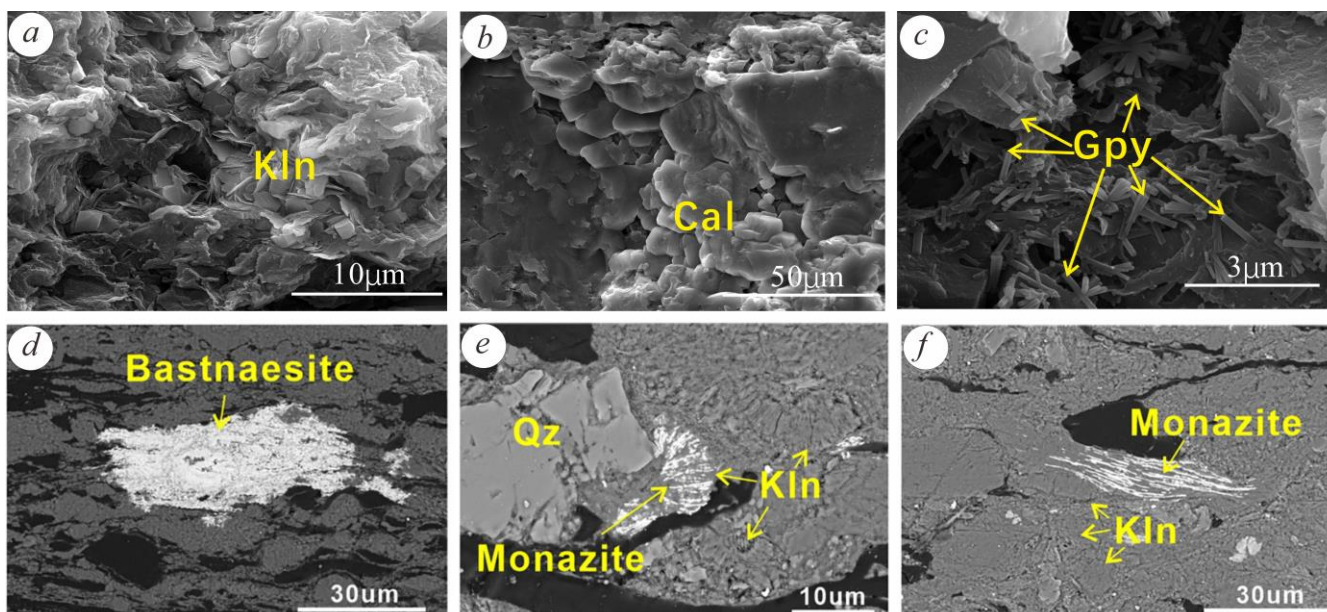


Figure 6. Scanning electron photomicrographs of minerals in Jungar coal. (a) Kaolinite (Kln), (b) calcite (Cal), and (c) gypsum (Gpy) in feed coal. (d) Bastnaesite in coal from the Haerwusu mine, (e,f) Monazite in coal from the Haerwusu mine.

Notes: (1) Feed coal was obtained from the Heidaigou coal mine; (2) panels (d–f) are from reference [35]. Qz, quartz.

3.3.2. Minerals in Coal Ash

The mineral types in bottom ash and fly ash were essentially the same but showed different relative contents. Specifically, the mullite, quartz, and gypsum contents of fly ash were slightly higher than those of bottom ash, while the amorphous mineraloid content of bottom ash was slightly higher than that of fly ash. Given that the density of hematite is

much higher than that of other minerals in coal combustion products, it was mainly present in bottom ash (Table 4, Figure 7).

Table 4. Mineral compositions of coal combustion products (%).

Sample	Mullite ($3\text{Al}_2\text{O}_3 \cdot 2\text{SiO}_2$)	Quartz (SiO_2)	Hematite (Fe_2O_3)	Gypsum ($\text{CaSO}_4 \cdot 2\text{H}_2\text{O}$)	Amorphous Solid
Bottom ash	16.3	6.9	4.7	1.1	71.0
Fly ash	19.8	7.1	1.5	2.6	69.0

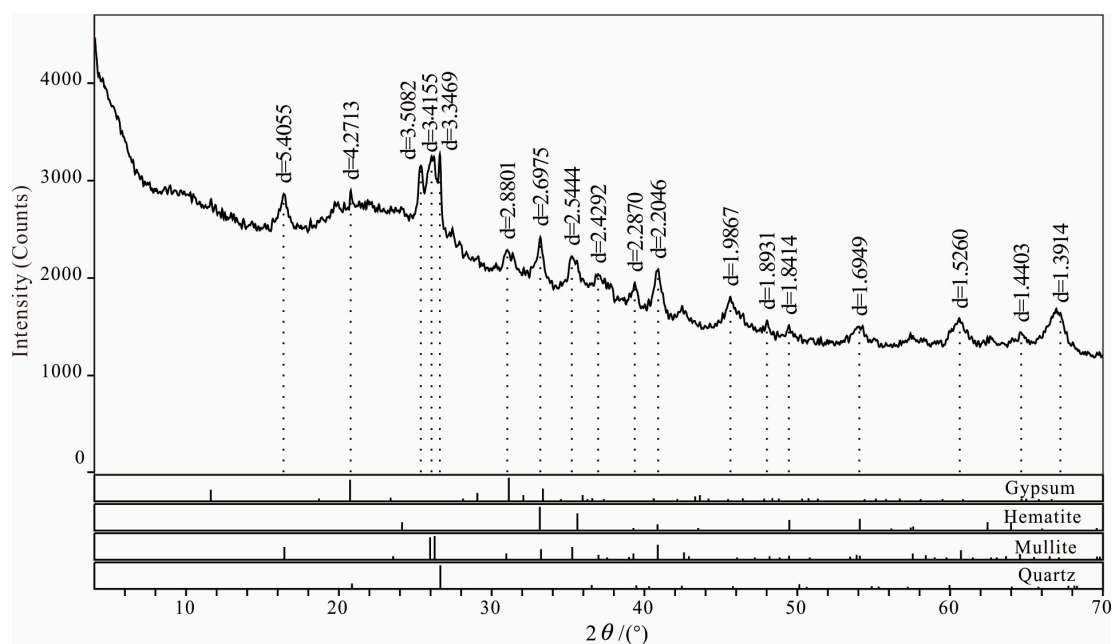


Figure 7. XRD spectrum of fly ash from the Jungar Energy Gangue Power Plant.

The mullite content of the coal ash samples from the Jungar Energy Gangue Power Plant was much lower than that of coal ash from the Jungar Power Plant (with a pulverized coal furnace at a combustion temperature of $1300\text{ }^{\circ}\text{C}$ – $1400\text{ }^{\circ}\text{C}$), which also uses Hedaigou coal as fuel [40,41]. Specifically, it varies in the range of 16.3%–19.8% (Table 4; Figure 7) and was approximately half that reported for the Jungar Power Plant (37.4%–34.9%) [41]. Further, the amorphous mineraloid content of the coal ash from the Jungar Energy Gangue Power Plant was 69%–71% (Table 4), whereas that of coal ash from the Jungar Power Plant was in the range of 52.6%–54.8% [41]. These differences could be attributed to kaolinite, the main mineral in the feed coal, which was transformed into amorphous metakaolin at $400\text{ }^{\circ}\text{C}$, and thereafter, metakaolin was gradually transformed into mullite at $900\text{ }^{\circ}\text{C}$ [54,55]. Therefore, the presence of mullite in the coal ash samples was possibly caused by the temperature exceeding $900\text{ }^{\circ}\text{C}$ during the combustion process. Furthermore, given that kaolinite is mainly converted into amorphous metakaolin, the amorphous solid contents of our samples were higher than those of the coal products of the Jungar Power Plant.

Scanning electron microscopy was employed to investigate the morphology of fly ash (Figure 8). Overall, the fly ash was composed of particles with irregular shapes and sizes (Figure 8a), mainly comprising Si–Al minerals [40,41,55,56]. Spherical iron silicate minerals were also observed (Figure 8b), and during combustion, the iron compounds in the coal possibly reacted with the silicates in the coal ash to form low-melting iron silicate fly ash particles [54,57]. Unburned carbon particles (Figure 8c) and zircons with good crystal shapes (Figure 8d) were also identified.

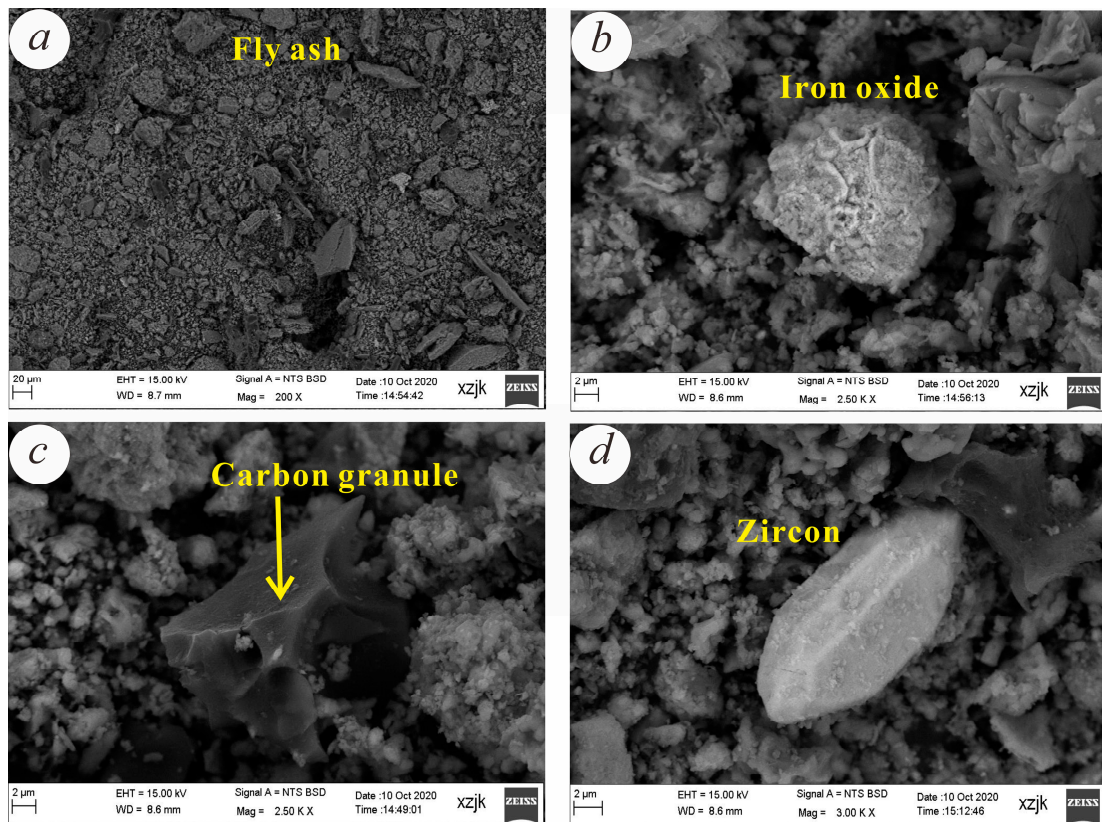


Figure 8. Scanning electron photomicrographs of fly ash. (a) Overall appearance of fly ash from the Jungar Energy Gangue Power Plant, (b) iron silicate minerals, (c) carbon granule, (d) zircon.

3.3.3. Modes of Occurrence of REEs

SEM-EDS was employed to observe REE fluoro-oxides and monazite in the fly ash samples (Figure 9, Table 5). The mode of occurrence of REEs in the coal ash was closely related to that in raw coal. Seredin and Dai [58] and Crowley [59] suggested that REEs in coal may occur (1) within primary minerals, such as monazite and xenotime, from the source area or volcanic ash; (2) within authigenic minerals, such as lanthanite, parisite, and bastnaesite, after diagenesis; (3) within organic matter [60,61]; and (4) as adsorbed ions. In general, the mineral properties of the source or volcanic ash were stable, as evidenced by the existence of monazite (Figure 9c), showing its original mineral structure, even after combustion in the CFB boiler. Reportedly, REE minerals with low stability and REEs occurring in organic matter or as adsorbed ions are likely to enter the amorphous glass phase [55,56,62] after coal combustion.

Table 5. Weight and atomic percentages of elements shown in the EDS spectrum in Figure 9.

Element	C	O	F	Al	Si	P	S	Ca	Ag	La	Ce	Nd	Th	
Figure 7a	Wt.%	9.80	27.67	8.44	5.95	3.57	\	0.68	2.87	\	4.86	14.90	7.20	14.07
	At.%	22.16	46.98	12.06	5.99	3.45	\	0.57	1.94	\	0.95	2.89	1.36	1.65
Figure 7b	Wt.%	8.26	57.79	\	15.63	16.70	1.62	\	\	\	\	\	\	\
	At.%	12.47	65.51	\	10.50	10.79	0.73	\	\	\	\	\	\	\
Figure 7c	Wt.%	9.70	46.37	0.77	7.11	6.80	6.60	\	0.28	1.15	6.10	12.06	3.06	\
	At.%	17.43	62.56	0.87	5.69	5.23	4.60	\	0.15	0.20	0.95	1.86	0.46	\

Notes: “\” indicates no data.

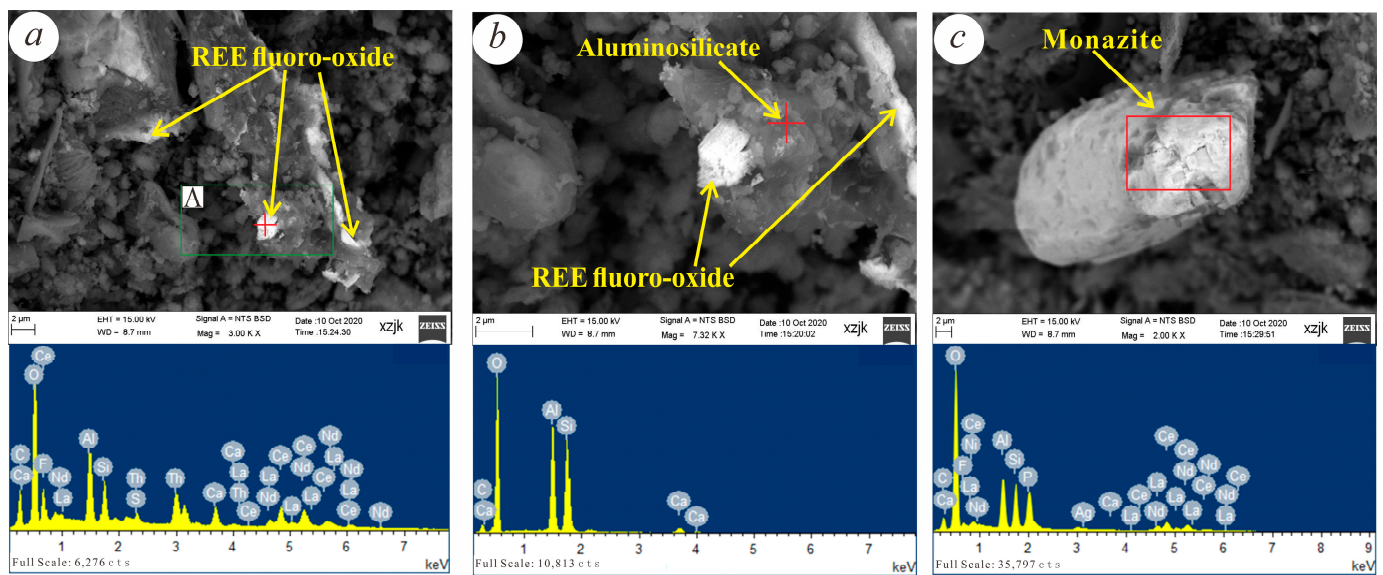
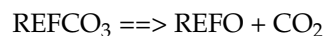


Figure 9. Scanning electron photomicrographs (BSD) and energy-dispersive spectroscopy of REE minerals in fly ash. (a) Rare earth element fluoro-oxides attached to the edges of aluminosilicates, with the accompanying energy spectrum; (b) enlargement of boxed area in Figure 7a, with the accompanying aluminosilicate energy spectrum; (c) monazite in fly ash, with the accompanying energy spectrum.

3.3.4. Minerals of Rare Earth Elements

Previous studies have shown that REEs in coal mainly occur in carbonates (kimurite, lanthanite, and bastnaesite), sulfates, phosphates (monazite, xenotime, and apatite), and silicates (clay and zircon) and can also occur in symbiosis with organic matter [63–68]. Jiu et al. [35] discovered REE minerals, such as monazite and bastnaesite, in coal from the Haerwusu mine (Figure 6d–f), which is adjacent to the Hedaigou mine (Figure 1).

The bright parts in the SEM images of the fly ash sample from the Jungar Energy Ganguge Power Plant were identified as REE minerals (Figure 9). Specifically, the minerals in Figure 9a mainly contained F, La, Ce, and Nd at the concentrations of 12.06, 0.95, 2.89, and 1.36 at.%, respectively, and were inferred to be REE fluoro-oxides [69–78], produced via the conversion of bastnaesite in boilers at high temperatures. Reportedly, fluorine in bastnaesite can be removed [70,71] to obtain REOs via roasting at 800 °C in humid air (60% humidity) with water participating in the reaction. However, this does not satisfy the humidity requirements for coal-fired boilers. When roasting is performed in dry air (at 800 °C), cerium fluoride minerals undergo the following reaction [70,71]:



This reaction results in the formation of a new rare earth fluoro-oxide (REFO) that is chemically stable [77,78] and can exist independently. Additionally, owing to the release of CO₂ during the reaction process, the molecular structure of REFO may be damaged, i.e., fractured at the reaction position such that it appears to exist at the mineral edge (Figure 9a,b).

The minerals shown in Figure 9c, which were inferred to be monazite minerals, mainly contained P, La, Ce, and Nd at the concentrations of 4.5, 0.95, 1.86, and 0.46 at.%, respectively [69]. The two REE mineral types observed via SEM showed different morphological characteristics for the coal ash: the REFO particles appeared small (size approximately 1 µm) and adhered to the edges of the main aluminosilicate minerals of fly ash, while monazite appeared relatively large (size approximately 20 µm) and existed independently in a granular form in bottom ash. These differences may be related to the behavioral characteristics of the two minerals during the combustion process. Monazite has good thermal stability [74]; hence, in the combustion process of the CFB boiler, where the tem-

perature generally does not exceed 1000 °C, the structure and properties of monazite do not change [70,71].

4. Conclusions

- (1) The REE content in the feed coal of the Jungar Energy Gangue Power Plant was found to be 198 µg/g, slightly higher than the average REE content for global coal. After combustion in a CFB boiler, the REE content of coal ash was markedly concentrated, and there was an evident difference in the distribution of the REEs between fly ash and bottom ash. Additionally, the extraction and utilization of REEs from fly ash did not require exploration and mining costs; hence, such ash has development and utilization value for REE extraction.
- (2) The mullite, quartz, calcite, and gypsum contents of fly ash were slightly higher than those of bottom ash, whereas amorphous solids were slightly more abundant in bottom ash than in fly ash. Compared with previously reported findings, this study showed that combustion temperature had a more significant effect on the mullite and amorphous mineraloid contents of coal ash.
- (3) Monazite in fly ash mainly existed in the form of particles that likely originated from raw coal, and its mineral structure did not change during coal combustion. Further, we observed that REE fluoro-oxides can be obtained from bastnaesite during combustion.

Author Contributions: Conceptualization, S.H. and S.N.; resources, S.N. and D.Z.; formal analysis, X.X., X.Y. and K.L.; writing—original draft preparation, S.H.; writing—review and editing, S.H. and Y.C.; supervision, S.N. All authors have read and agreed to the published version of the manuscript.

Funding: This research was funded by the National Key R&D Program of China (2021YFC2902005), the Xinjiang Province Major Science and Technology Project (2022A03014-2), and the China Coal Geological Administration Carbon Neutral Special Project (ZMKJ-2021-ZX03-01).

Data Availability Statement: The data obtained and analyzed within the framework of this study are available from the corresponding author upon reasonable request.

Conflicts of Interest: The authors declare no conflict of interest.

References

1. Zhai, M.; Wu, F.; Hu, R.; Jiang, S.; Li, W.; Wang, R.; Wang, D.; Qi, T.; Qing, K.; Wen, H. Critical metal mineral resources: Current research status and scientific issues. *Bull. Natl. Nat. Sci. Fdn. China*. **2019**, *33*, 106–111, (In Chinese with English abstract).
2. Yin, J.; Song, X. A review of major rare earth element and yttrium deposits in China. *Aus. J. Earth Sci.* **2022**, *4*, 1–25. [[CrossRef](#)]
3. Balam, V. Potential Future Alternative Resources for Rare Earth Elements: Opportunities and Challenges. *Minerals* **2023**, *13*, 425. [[CrossRef](#)]
4. National Minerals Information Center. *Geological Survey Mineral Commodity Summaries 2023 Data Release: U.S. Geological Survey Data Release*; USGS: Reston, VA, USA, 2023. [[CrossRef](#)]
5. Liu, X.; Zhang, H.; Tang, Y.; Liu, Y. REE Geochemical Characteristic of Apatite: Implications for Ore Genesis of the Zhijin Phosphorite. *Minerals* **2020**, *10*, 1012. [[CrossRef](#)]
6. Dai, S.; Yang, J.; Ward, C.R.; Hower, J.C.; Liu, H.; Garrison, T.M.; French, D.; O’Keefe, J.M.K. Geochemical and mineralogical evidence for a coal-hosted uranium deposit in the Yili Basin, Xinjiang, northwestern China. *Ore Geol. Rev.* **2015**, *70*, 1–30. [[CrossRef](#)]
7. Dai, S.; Ward, C.R.; Graham, I.T.; French, D.; Hower, J.C.; Zhao, L.; Wang, X. Altered volcanic ashes in coal and coal-bearing sequences: A review of their nature and significance. *Earth-Sci. Rev.* **2017**, *175*, 44–74. [[CrossRef](#)]
8. Dai, S.; Yan, X.; Ward, C.R.; Hower, J.C.; Zhao, L.; Wang, X.; Zhao, L.; Ren, D.; Finkelman, R.B. Valuable elements in Chinese coals: A review. *Int. Geol. Rev.* **2018**, *60*, 590–620. [[CrossRef](#)]
9. Dai, S.; Finkelman, R.B.; French, D.; Hower, J.C.; Graham, I.T.; Zhao, F. Modes of occurrence of elements in coal: A critical evaluation. *Earth-Sci. Rev.* **2021**, *222*, 103815. [[CrossRef](#)]
10. Hower, J.C.; Berti, D.; Hochella, M.F.; Mardon, S.M. Rare earth minerals in a “no tonstein” section of the Dean (Fire Clay) coal, Knox County, Kentucky. *Int. J. Coal Geol.* **2018**, *193*, 73–86. [[CrossRef](#)]
11. Hower, J.C.; Eble, C.F.; Mastalerz, M. Petrology of the Fire Clay coal, Bear Branch, Perry County, Kentucky. *Int. J. Coal Geol.* **2022**, *249*, 103891. [[CrossRef](#)]
12. Ma, M.; Wang, W.; Li, J.; Zhang, K.; He, X. Experimental Study of the Activation Effect of Oxalic Acid on the Dissolution of Rare Earth Elements in the Typical Diagenetic Minerals of Coal Seams. *Minerals* **2023**, *13*, 525. [[CrossRef](#)]

13. Chatterjee, S.; Mastalerz, M.; Drobniak, A.; Karacan, C.Ö. Machine learning and data augmentation approach for identification of rare earth element potential in Indiana Coals, USA. *Int. J. Coal Geol.* **2022**, *259*, 104054. [[CrossRef](#)]
14. Chitlango, F.Z.; Wagner, N.J.; Moroeng, O.M. Characterization and pre-concentration of rare earth elements in density fractionated samples from the Waterberg Coalfield, South Africa. *Int. J. Coal Geol.* **2023**, *275*, 104299. [[CrossRef](#)]
15. Di, S.; Dai, S.; Nechaev, V.P.; Zhang, S.; French, D.; Graham, I.T.; Spiro, B.; Finkelman, R.B.; Hou, Y.; Wang, Y.; et al. Granite-bauxite provenance of abnormally enriched boehmite and critical elements (Nb, Ta, Zr, Hf and Ga) in coals from the Eastern Surface Mine, Ningwu Coalfield, Shanxi Province, China. *J. Geochem. Explor.* **2022**, *239*, 107016. [[CrossRef](#)]
16. Liu, J.; Spiro, B.F.; Dai, S.; French, D.; Graham, I.T.; Wang, X.; Zhao, L.; Zhao, J.; Zeng, R. Strontium isotopes in high- and low-Ge coals from the Shengli Coalfield, Inner Mongolia, northern China: New indicators for Ge source. *Int. J. Coal Geol.* **2021**, *233*, 103642. [[CrossRef](#)]
17. Hower, J.C.; Warwick, P.D.; Scanlon, B.R.; Reedy, R.C.; Childress, T.M. Distribution of rare earth and other critical elements in lignites from the Eocene Jackson Group, Texas. *Int. J. Coal Geol.* **2023**, *275*, 104302. [[CrossRef](#)]
18. Shen, M.; Dai, S.; French, D.; Graham, I.T.; Spiro, B.F.; Wang, N.; Tian, X. Geochemical and mineralogical evidence for the formation of siderite in late Permian coal-bearing strata from western Guizhou, SW China. *Chem. Geol.* **2023**, *637*, 121675. [[CrossRef](#)]
19. Shen, M.; Dai, S.; Graham, I.T.; Nechaev, V.P.; French, D.; Zhao, F.; Shao, L.; Liu, S.; Zuo, J.; Zhao, J.; et al. Mineralogical and geochemical characteristics of altered volcanic ashes (tonsteins and K-bentonites) from the latest Permian coal-bearing strata of western Guizhou Province, southwestern China. *Int. J. Coal Geol.* **2021**, *237*, 103707. [[CrossRef](#)]
20. Wang, N.; French, D.; Dai, S.; Graham, I.T.; Zhao, L.; Song, X.; Zheng, J.; Gao, Y.; Wang, Y. Origin of chamosite and berthierine: Implications for volcanic-ash-derived Nb-Zr-REY-Ga mineralization in the Lopingian sequences from eastern Yunnan, SW China. *J. Asian Earth Sci.* **2023**, *253*, 105703. [[CrossRef](#)]
21. Zhou, C.; Li, C.; Li, W.; Sun, J.; Li, Q.; Wu, W.; Liu, G. Distribution and preconcentration of critical elements from coal fly ash by integrated physical separations. *Int. J. Coal Geol.* **2022**, *261*, 104095. [[CrossRef](#)]
22. Strzałkowska, E. Rare earth elements and other critical elements in the magnetic fraction of fly ash from several Polish power plants. *Int. J. Coal Geol.* **2022**, *258*, 104015. [[CrossRef](#)]
23. Wang, Q.; Dai, S.; French, D.; Spiro, B.; Graham, I.; Liu, J. Hydrothermally-altered coal from the Daqingshan Coalfield, Inner Mongolia, northern China: Evidence from stable isotopes of C within organic matter and C-O-Sr in associated carbonates. *Int. J. Coal Geol.* **2023**, *276*, 104330. [[CrossRef](#)]
24. Yang, P.; Dai, S.; Nechaev, V.P.; Song, X.; Yu Chekryzhov, I.; Tarasenko, I.A.; Tian, X.; Yao, M.; Kang, S.; Zheng, J. Modes of occurrence of critical metals (Nb-Ta-Zr-Hf-REY-Ga) in altered volcanic ashes in the Xuanwei Formation, eastern Yunnan Province, SW China: A quantitative evaluation based on sequential chemical extraction. *Ore Geol. Rev.* **2023**, *160*, 105617. [[CrossRef](#)]
25. Arbuzov, S.I.; Chekryzhov, I.Y.; Verkhoturov, A.A.; Spears, D.A.; Melkiy, V.A.; Zarubina, N.V.; Blokhin, M.G. Geochemistry and rare-metal potential of coals of the Sakhalin coal basin, Sakhalin island, Russia. *Int. J. Coal Geol.* **2023**, *268*, 104197. [[CrossRef](#)]
26. Arnold, B.J. A review of element partitioning in coal preparation. *Int. J. Coal Geol.* **2023**, *274*, 104296. [[CrossRef](#)]
27. Nechaev, V.P.; Dai, S.; Chekryzhov, I.Y.; Tarasenko, I.A.; Zin'kov, A.V.; Moore, T.A. Origin of the tuff parting and associated enrichments of Zr, REY, redox-sensitive and other elements in the Early Miocene coal of the Siniy Utyes Basin, southwestern Primorye, Russia. *Int. J. Coal Geol.* **2022**, *250*, 103913. [[CrossRef](#)]
28. Hou, Y.; Dai, S.; Nechaev, V.P.; Finkelman, R.B.; Wang, H.; Zhang, S.; Di, S. Mineral matter in the Pennsylvanian coal from the Yangquan Mining District, northeastern Qinshui Basin, China: Enrichment of critical elements and a Se-Mo-Pb-Hg assemblage. *Int. J. Coal Geol.* **2023**, *266*, 104178. [[CrossRef](#)]
29. Moore, T.A.; Dai, S.; Huguet, C.; Pearse, J.; Liu, J.; Esterle, J.S.; Jia, R. Petrographic and geochemical characteristics of selected coal seams from the Late Cretaceous-Paleocene Guaduas Formation, Eastern Cordillera Basin, Colombia. *Int. J. Coal Geol.* **2022**, *259*, 104042. [[CrossRef](#)]
30. Ning, S.; Huang, S.; Zhu, S.; Zhang, W.; Deng, X.; Li, C.; Qiao, J.; Zhang, J.; Zhang, N. Mineralization zoning of coal-metal deposits in China. *Sci. Bull.* **2019**, *64*, 2501–2513, (In Chinese with English abstract). [[CrossRef](#)]
31. Dai, S.; Li, D.; Chou, C.-L.; Zhao, L.; Zhang, Y.; Ren, D.; Ma, Y.; Sun, Y. Mineralogy and geochemistry of boehmite-rich coals: New insights from the Haerwusu Surface Mine, Jungar Coalfield, Inner Mongolia, China. *Int. J. Coal Geol.* **2008**, *74*, 185–202. [[CrossRef](#)]
32. Dai, S.; Jiang, Y.; Ward, C.R.; Gu, L.; Seredin, V.V.; Liu, H.; Zhou, D.; Wang, X.; Sun, Y.; Zou, J.; et al. Mineralogical and geochemical compositions of the coal in the Guanbanwusu Mine, Inner Mongolia, China: Further evidence for the existence of an Al (Ga and REE) ore deposit in the Jungar Coalfield. *Int. J. Coal Geol.* **2012**, *98*, 10–40. [[CrossRef](#)]
33. Xiao, L.; Zhao, B.; Duan, P.; Shi, Z.; Ma, J.; Lin, M. Geochemical Characteristics of Trace Elements in the No. 6 Coal Seam from the Chuancaogedan Mine, Jungar Coalfield, Inner Mongolia, China. *Minerals* **2016**, *6*, 28. [[CrossRef](#)]
34. Li, J.; Zhang, S.; Wang, H.; Xie, X. Geochemical Characteristics of Critical Metal Elements in the No. 9 Coal Seam from the Xinyuan Mine, Northern Qinshui Coalfield, Shanxi Province, China. *Minerals* **2023**, *13*, 278. [[CrossRef](#)]
35. Jiu, B.; Huang, W.; Spiro, B.; Hao, R.; Mu, N.; Wen, L.; Hao, H. Distribution of Li, Ga, Nb, and REEs in coal as determined by LA-ICP-MS imaging: A case study from Jungar coalfield, Ordos Basin, China. *Int. J. Coal Geol.* **2023**, *267*, 104184. [[CrossRef](#)]
36. Kanesalingam, B.; Fernando, W.A.M.; Panda, S.; Jayawardena, C.; Attygalle, D.; Amarasinghe, D.A.S. Harnessing the Capabilities of Microorganisms for the Valorisation of Coal Fly Ash Waste through Biometallurgy. *Minerals* **2023**, *13*, 724. [[CrossRef](#)]
37. Alterary, S.; Marei, N.H. The Impact of Coal Fly Ash Purification on Its Antibacterial Activity. *Minerals* **2020**, *10*, 1002. [[CrossRef](#)]

38. Liu, H.; Sun, Q.; Wang, B.; Wang, P.; Zou, J. Morphology and Composition of Microspheres in Fly Ash from the Luohuang Power Plant, Chongqing, Southwestern China. *Minerals* **2016**, *6*, 30. [[CrossRef](#)]
39. Srivastava, R.R.; Rajak, D.K.; Ilyas, S.; Kim, H.; Pathak, P. Challenges, Regulations, and Case Studies on Sustainable Management of Industrial Waste. *Minerals* **2023**, *13*, 51. [[CrossRef](#)]
40. Dai, S.; Zhao, L.; Peng, S.; Chou, C.; Wang, X.; Zhang, Y.; Li, D.; Sun, Y. Abundances and distribution of minerals and elements in high-alumina coal fly ash from the Jungar Power Plant, Inner Mongolia, China. *Int. J. Coal Geol.* **2010**, *81*, 320–332. [[CrossRef](#)]
41. Zhao, L.; Dai, S.; Zhang, Y.; Wang, X.; Li, D.; Lu, Y.; Zhu, X.; Sun, Y.; Ma, Y. Mineral abundances of high alumina fly ash from the Jungar Power Plant, Inner Mongolia, China. *J. China Coal Soc.* **2008**, *33*, 1168–1172, (In Chinese with English abstract).
42. Couch, G. *Understanding Slagging and Fouling in PF Combustion*; IEA Coal Research: London, UK, 1994.
43. Di, S.; Dai, S.; Nechaev, V.P.; French, D.; Graham, I.T.; Zhao, L.; Finkelman, R.B.; Wang, H.; Zhang, S.; Hou, Y. Mineralogy and enrichment of critical elements (Li and Nb-Ta-Zr-Hf-Ga) in the Pennsylvanian coals from the Antaibao Surface Mine, Shanxi Province, China: Derivation of pyroclastics and sediment-source regions. *Int. J. Coal Geol.* **2023**, *273*, 104262. [[CrossRef](#)]
44. Xu, F.; Qin, S.; Li, S.; Wen, H.; Lv, D.; Wang, Q.; Kang, S. The migration and mineral host changes of lithium during coal combustion: Experimental and thermodynamic calculation study. *Int. J. Coal Geol.* **2023**, *275*, 104298. [[CrossRef](#)]
45. Zhang, S.; Xiu, W.; Sun, B.; Liu, Q. Provenance of multi-stage volcanic ash recorded in the Late Carboniferous coal in the Jungar Coalfield, North China, and their contribution to the enrichment of critical metals in the coal. *Int. J. Coal Geol.* **2023**, *273*, 104265. [[CrossRef](#)]
46. Zhang, Z.; Lv, D.; Hower, J.C.; Wang, L.; Shen, Y.; Zhang, A.; Xu, J.; Gao, J. Geochronology, mineralogy, and geochemistry of tonsteins from the Pennsylvanian Taiyuan Formation of the Jungar Coalfield, Ordos Basin, North China. *Int. J. Coal Geol.* **2023**, *267*, 104183. [[CrossRef](#)]
47. Sun, Y.; Zhao, C.; Qin, S.; Xiao, L.; Li, Z.; Lin, M. Occurrence of some valuable elements in the unique “high-aluminium coals” from the Jungar coalfield, China. *Ore Geol. Rev.* **2016**, *72*, 659–668. [[CrossRef](#)]
48. Liu, D.; Gao, G.; Chi, J.; Wang, Y.; Guo, Z. Distribution Rule of Rare Earth and Trace Elements in the Heidaigou Openpit Coal Mine in the Jungar Coal Field. *Acta Geol. Sin.* **2018**, *92*, 2368–2375, (In Chinese with English abstract).
49. Liu, D.; Zhou, A.; Zeng, F.; Zhao, F.; Zou, Y. The Petrography, Mineralogy and Geochemistry of Some Cu- and Pb-Enriched Coals from Jungar Coalfield, Northwestern China. *Minerals* **2018**, *8*, 5. [[CrossRef](#)]
50. Dai, S.; Seredin, V.V.; Ward, C.R.; Hower, J.C.; Xing, Y.; Zhang, W.; Song, W.; Wang, P. Enrichment of U–Se–Mo–Re–V in coals preserved within marine carbonate successions: Geochemical and mineralogical data from the Late Permian Guiding Coalfield, Guizhou, China. *Miner. Depos.* **2015**, *50*, 159–186. [[CrossRef](#)]
51. Ketris, M.P.; Yudovich, Y.E. Estimations of Clarkes for Carbonaceous Biolithes: World Averages for Trace Element Contents in Black Shales and Coals. *Int. J. Coal Geol.* **2009**, *78*, 135–148. [[CrossRef](#)]
52. Ruud, M. Trace element behavior in coal-fired power plants. *Fuel Process. Technol.* **1994**, *39*, 199–217. [[CrossRef](#)]
53. Dai, S.; Ren, D.; Chou, C.-L.; Li, S.; Jiang, Y. Mineralogy and geochemistry of the No. 6 Coal (Pennsylvanian) in the Junger Coalfield, Ordos Basin, China. *Int. J. Coal Geol.* **2006**, *66*, 253–270. [[CrossRef](#)]
54. Gerald, P.H.; Frank, E.H.; George, R.D. Investigation of the high-temperature behaviour of coal ash in reducing and oxidizing atmospheres. *Fuel* **1981**, *60*, 585–597. [[CrossRef](#)]
55. Hower, J.C.; Groppo, J.G.; Joshi, P.; Dai, S.; Moecher, D.P.; Johnston, M.N. Location of Cerium in Coal-Combustion Fly Ashes: Implications for Recovery of Lanthanides. *Coal Combust. Gasif. Prod.* **2013**, *5*, 73–78. [[CrossRef](#)]
56. Dai, S.; Zhao, L.; Hower, J.C.; Johnston, M.N.; Song, W.; Wang, P.; Zhang, S. Petrology, mineralogy, and chemistry of size-fractioned fly ash from the Jungar power plant, Inner Mongolia, China, with emphasis on the distribution of rare earth elements. *Energy Fuels* **2014**, *28*, 1502–1514. [[CrossRef](#)]
57. Rohatgi, P.K.; Guo, R.Q.; Iksan, H.; Borchelt, E.J.; Asthana, R. Pressure infiltration technique for synthesis of aluminum–fly ash particulate composite. *Mater. Sci. Eng. A* **1998**, *244*, 22–30. [[CrossRef](#)]
58. Seredin, V.V.; Dai, S. Coal deposits as potential alternative sources for lanthanides and yttrium. *Int. J. Coal Geol.* **2012**, *94*, 67–93. [[CrossRef](#)]
59. Crowley, S.S.; Stanton, R.W.; Ryer, T.A. The effects of volcanic ash on the maceral and chemical composition of the C coal bed, Emery Coal Field, Utah. *Org. Geochem.* **1989**, *14*, 315–331. [[CrossRef](#)]
60. Seredin, V.V. Rare earth elements in germanium-bearing coal seams of the Spetsugli Deposit (Primor’e Region, Russia). *Geol. Ore Depos.* **2005**, *47*, 238–255.
61. Huang, S.; Ning, S.; Zhang, J.; Zhang, L.; Liu, K. REE characteristics of the coal in the Erlan Basin, Inner Mongolia, China, and its economic value. *China Geol.* **2021**, *4*, 256–265. [[CrossRef](#)]
62. Kolker, A.; Scott, C.; Hower, J.C.; Vazquez, J.A.; Christina, L.L.; Dai, S. Distribution of rare earth elements in coal combustion fly ash, determined by SHRIMP-RG ion microprobe. *Int. J. Coal Geol.* **2017**, *184*, 1–10. [[CrossRef](#)]
63. Chen, J.; Chen, P.; Yao, D.; Liu, Z.; Wu, Y.; Liu, W.; Hu, Y. Mineralogy and geochemistry of late Permian coals from the Donglin Coal Mine in the Nantong coalfield in Chongqing, southwestern China. *Int. J. Coal Geol.* **2015**, *149*, 24–40. [[CrossRef](#)]
64. Dai, S.; Finkelman, R.B. Coal as a promising source of critical elements: Progress and future prospects. *Int. J. Coal Geol.* **2018**, *186*, 155–164. [[CrossRef](#)]
65. Dai, S.; Hower, J.C.; Finkelman, R.B.; Graham, I.T.; French, D.; Ward, C.R.; Eskenazy, G.; Wei, Q.; Zhao, L. Organic associations of non-mineral elements in coal: A review. *Int. J. Coal Geol.* **2020**, *218*, 103347. [[CrossRef](#)]

66. Finkelman, R.B.; Dai, S.; French, D. The importance of minerals in coal as the hosts of chemical elements: A review. *Int. J. Coal Geol.* **2019**, *212*, 103251. [[CrossRef](#)]
67. Duan, P.; Wang, W.; Sang, S.; Tang, Y.; Ma, M.; Zhang, W.; Liang, B. Geochemistry of Toxic Elements and Their Removal via the Preparation of High-Uranium Coal in Southwestern China. *Minerals* **2018**, *8*, 83. [[CrossRef](#)]
68. Hower, J.C.; Eble, C.F.; Backus, J.S.; Xie, P.; Liu, J.; Fu, B.; Hood, M.M. Aspects of rare earth element enrichment in Central Appalachian coals. *Appl. Geochem.* **2020**, *120*, 104676. [[CrossRef](#)]
69. Huang, L.H. *Extraction Technology of Rare Earth*; Metallurgical Industry Press: Beijing, China, 2006. (In Chinese)
70. Sun, S.; Wu, Z.; Gao, B.; Bian, X.; Wu, W.; Tu, G. Effect of CaO on Fluorine in the Decomposition of REFCO₃. *J. Rare Earths.* **2007**, *25*, 508–511. [[CrossRef](#)]
71. Wu, Z.; Sun, S.; Wu, W.; Bian, X.; Tu, G. Effect of air humidity on fluorine escape during bastnaesite roasting. *Chin. Rare Earth.* **2008**, *5*, 1–4, (In Chinese with English abstract).
72. Dai, S.; Ren, D.; Chou, C.-L.; Finkelman, R.; Seredin, V.V.; Zhou, Y. Geochemistry of trace elements in Chinese coals: A review of abundances, genetic types, impacts on human health, and industrial utilization. *Int. J. Coal Geol.* **2012**, *94*, 3–21. [[CrossRef](#)]
73. Dai, S.; Ren, D.; Zhou, Y.; Chou, C.-L.; Wang, X.; Zhao, L.; Zhu, X. Mineralogy and geochemistry of a superhigh-organic-sulfur coal, Yanshan Coalfield, Yunnan, China: Evidence for a volcanic ash component and influence by submarine exhalation. *Chem. Geol.* **2008**, *255*, 182–194. [[CrossRef](#)]
74. Dai, S.; Wang, X.; Seredin, V.V.; Hower, J.C.; Ward, C.R.; O’Keefe, J.M.K.; Huang, W.; Li, T.; Li, X.; Liu, H.; et al. Petrology, mineralogy, and geochemistry of the Ge-rich coal from the Wulantuga Ge ore deposit, Inner Mongolia, China: New data and genetic implications. *Int. J. Coal Geol.* **2012**, *90*, 72–99. [[CrossRef](#)]
75. Dai, S.; Wang, X.; Zhou, Y.; Hower, J.C.; Li, D.; Chen, W.; Zhu, X.; Zou, J. Chemical and mineralogical compositions of silicic, mafic, and alkali tonsteins in the late Permian coals from the Songzao Coalfield, Chongqing, Southwest China. *Chem. Geol.* **2011**, *282*, 29–44. [[CrossRef](#)]
76. Dai, S.; Zou, J.; Jiang, Y.; Ward, C.R.; Wang, X.; Li, T.; Xue, W.; Liu, S.; Tian, H.; Sun, X.; et al. Mineralogical and geochemical compositions of the Pennsylvanian coal in the Adaohai Mine, Daqingshan Coalfield, Inner Mongolia, China: Modes of occurrence and origin of diaspore, gorceixite, and ammonian illite. *Int. J. Coal Geol.* **2012**, *94*, 250–270. [[CrossRef](#)]
77. Shahbaz, A. A systematic review on leaching of rare earth metals from primary and secondary sources. *Miner. Eng.* **2022**, *184*, 107632. [[CrossRef](#)]
78. Kumari, A.; Panda, R.; Kumar, M.; Kumar, J.R.; Lee, J.Y. Process development to recover rare earth metals from monazite mineral: A review. *Miner. Eng.* **2015**, *79*, 102–115. [[CrossRef](#)]

Disclaimer/Publisher’s Note: The statements, opinions and data contained in all publications are solely those of the individual author(s) and contributor(s) and not of MDPI and/or the editor(s). MDPI and/or the editor(s) disclaim responsibility for any injury to people or property resulting from any ideas, methods, instructions or products referred to in the content.